Published in final edited form as:
Exp Cell Res. 2010 August 15; 316(14): 2322–2339. doi:10.1016/j.yexcr.2010.05.020.

Syndecan-1 Regulates Cell Migration and Fibronectin Fibril Assembly

Mary Ann Stepp[1,2,*], **William P. Daley**[3], **Audrey M. Bernstein**[4], **Sonali Pal-Ghosh**[1], **Gauri Tadvalkar**[1], **Alexey Shashurin**[1], **Sarah Palsen**[1], **Rosalyn A. Jurjus**[5], and **Melinda Larsen**[3]

[1]Department of Anatomy and Regenerative Biology, George Washington University Medical Center, Washington DC 20037, USA

[2]Department of Ophthalmology, George Washington University Medical Center, Washington DC 20037, USA

[3]Department of Biological Sciences, University at Albany, State University of New York, Albany, NY 12222, USA

[4]Department of Ophthalmology, Mount Sinai School of Medicine, New York, NY 100029, USA

[5]Department of Microbiology and Tropical Medicine, George Washington University Medical Center, Washington DC 20037, USA

Abstract

Corneal scarring is a major cause of blindness worldwide and can result from the deposition of abnormal amounts of collagen fibers lacking the correct size and spacing required to produce a clear cornea. Collagen fiber formation requires a preformed fibronectin (FN) matrix. We demonstrate that the loss of syndecan1 (sdc1) in corneal stromal cells (CSC) impacts cell migration rates, the sizes and composition of focal and fibrillar adhesions, the activation of integrins, and the assembly of fibronectin into fibrils. Integrin and fibronectin expression are not altered on sdc1 null CSCs. Cell adhesion, spreading, and migration studies using low compared to high concentrations of FN and collagen I (CNI) or vitronectin (VN) with and without activation of integrins by manganese chloride show that the impact of sdc1 depletion on integrin activation varies depending on the integrin-mediated activity evaluated. Differences in FN-fibrillogenesis and migration in sdc1 null CSCs are reversed by addition of manganese chloride but cell spreading differences remain. To determine if our findings on sdc1 were specific to the cornea, we compared the phenotypes of sdc1 null dermal fibroblasts with those of CSCs. We found that without sdc1, both cell types migrate faster; however, cell-type specific differences in FN expression and its assembly into fibrils exist between these two cell types. Together, our data demonstrate that sdc1 functions to regulate integrin activity in multiple cell types. Loss of sdc1-mediated integrin function results in cell-type specific differences in matrix assembly. A better understanding of how different cell types regulate FN fibril formation via syndecans and integrins will lead to better treatments for scarring and fibrosis.

*Communicating author's address: Mary Ann Stepp, Ph.D., Dept. Anatomy and Regenerative Biology and Dept. of Ophthalmology, GWU Medical School, Ross Hall Room 226C, 2300 I St. NW, Washington, DC 20037 USA, 1-202-994-0557 (office), 1-202-994-0535 (lab), 1-202-994-8885 (fax), mastepp@gwu.edu.

Keywords

integrins; cell migration; fibronectin; corneal stromal cells

Introduction

Corneal clarity is an absolute requirement for vision. If the light waves bouncing off objects in our visual field cannot reach the retina due to an opaque cornea or are refracted as they pass through the cornea due to scars, vision fails. Keratan sulfate proteoglycans (including lumican) and dermatan sulfate proteoglycans (including biglycan and decorin) play important roles in mediating corneal clarity by regulating the diameter and spacing of collagen fibrils [1–3]. The major heparan sulfate proteoglycans (HSPGs) found in the cornea are perlecan, at the basement membrane zone [4] and syndecan-1 (sdc1). Sdc1 is abundant on epidermal keratinocytes and corneal epithelial cells [5] and expressed at low levels in the quiescent dermis and corneal stroma. In response to injury, sdc1 ectodomain is shed from epithelial cells and its expression is up-regulated in both epithelial cells and fibroblasts [6–9].

In vivo short-term skin and corneal wound healing studies on sdc 1 null mice demonstrated reduced healing rates [5] and in vitro studies showed that this was caused by increased epithelial cell-adhesion mediated by α6β4 and αv-containing integrins [10]. In vivo long-term skin cancer studies demonstrated that the sdc1 null mice develop fewer tumors with increased α6β4 integrin localization at the basement membrane zone [11]. Studies performed to assess the frequency of recurrent corneal erosions showed that sdc1 null mice had 50% fewer recurrent erosions when compared to wt mice six weeks after wounding [12]. Sdc1 null epithelial cells that are more adherent in vitro, migrate slower and reform stable adhesions more readily in vivo. In contrast to keratinocytes, the dermal fibroblasts (DFs) isolated from sdc1 null mice have increased migration rates [13]. While the differences between wt and sdc1 null mice in skin and corneal healing could be entirely due to differences in epithelial cell adhesion, both DFs and CSCs play vital roles in mediating tissue integrity in vivo and alterations in their function may contribute to these healing outcomes.

We set out to determine whether cells isolated from the corneal stroma show differences in cell migration and integrin function. The corneal stromal cells (CSCs) make the ordered collagen and proteoglycan extracellular matrix whose regular structure allows light to pass through without being bent and keeps the cornea transparent [14–19]. We show here that loss of sdc1 in CSCs impacts both cell migration and assembly of FN into fibrils. The sdc1 null CSCs have less of the activated ligand-bound form of the β1 integrin on their surface compared to wt CSCs but have the same amount of total β1 integrin on their surface. The rapid migration phenotype of sdc1 null corneal fibroblasts is reduced when cells are replated onto high concentrations of integrin ligands that induce integrin activation via outside-in signaling. Furthermore, we show that the differences in migration and FN-fibrillogenesis in sdc1 null CSCs can be reversed by addition of $MnCl_2$, a treatment that activates integrin function. Finally, although sdc1 null CSCs and DFs both migrate faster than wt cells on a variety of different substrates, we find cell type-specific differences in FN expression and its assembly into fibrils. These data suggest that sdc1 regulates FN fibrillogenesis, and that this function of sdc1 is cell-type specific.

Materials and Methods

Mouse Corneal Stromal Cell and Dermal Fibroblast Cell Culture

All animal protocols were approved by the GWU Animal Care and Use committee. Wt mice (BALB/c) were obtained from NCI-Frederick. Construction of sdc1 deficient mice was described previously [5]. Primary mouse dermal fibroblasts were isolated from newborn BALB/c or sdc1 null mice as described previously [13]. Corneal stromal cells were obtained from wt or sdc1 null mice at eight weeks of age. Mice were sacrificed, eyes enucleated and the corneal buttons were digested in 0.35% collagenase type I (267 U/mg CLS 1, #4198 210U/mg, Worthington Biochemical Corporation) at 37°C with occasional vigorous shaking; 20 ml of collagenase solution was used per 10 corneas for 90 minutes. Cells were released from the stroma by trituration, followed by filtration through a sterile 100 μm filter (BD Biosciences #352360). CSCs were centrifuged at 1000 rpm for five minutes, resuspended in complete fibroblast media containing 10% fetal calf serum, and plated out into 10 cm dishes. Media was changed every other day, and cells were passaged after achieving confluence. CSCs isolated after 3 passages were resuspended in freezing media [DMEM with 10% FCS, 1.4 mM calcium, 10% DMSO (ThermoFisher #20684), 10mM Hepes, pH=7.3] and stored in liquid nitrogen till needed. For each experiment, CSCs were grown in DMEM with 10% serum (unless indicated) and used between the 3rd and 4th passage. For replating studies, tissue culture plates were coated with a mixture of human plasma fibronectin and collagen I [FNCNI; 10 μg/ml human plasma fibronectin (BD Pharmingen #345008) and collagen I (1% collagen (PureCol INAMED Biomaterials, # 5409] or vitronectin [VN; 10 μg/ml human vitronectin, BD Pharmingen #354238] in serum-free media for 15 min at 37°C. For studies comparing cell migration of CSCs maintained in media containing 10% serum cells under quiescent conditions, defined media was prepared as described by Bernstein and colleagues [18].

Manual Corneal Debridement Wounding

The in vivo corneal wound healing experiments were conducted in voluntary compliance with the Association for Research in Vision and Ophthalmology Guidelines for the Use of Animals in Research and all procedures were approved by the GWU Animal Care and Use Committee. The technique has been previously described [20]. In brief, 7–8 week old mice were anesthetized, topical anesthetic applied to their ocular surface, and corneas scraped with a dull scalpel to remove the corneal epithelium. A 1.5 mm central corneal area was demarcated with a trephine and epithelial cells removed manually by gentle scraping with a dulled blade. After wounding, all eyes were treated with erythromycin ophthalmic ointment to minimize inflammation and keep the ocular surface moist while the mice were under anesthesia. This procedure has been determined previously to leave the basement membrane intact and non-denatured. Mice were sacrificed at 24 and 48 hours after injury and eyes fixed in 4% paraformaldehyde and processed for immunofluorescence microscopy as described previously [21].

Antibodies

These studies required primary antibodies which were obtained from various sources. Table 1 shows the names, sources, and applications used for each primary antibody used. Secondary antibodies were obtained from Molecular Probes and Jackson Immunosciences as described previously [10].

Immunostaining

We were concerned that the αv integrin and vinculin primary antibodies when bound to focal adhesions might prevent access to focal adhesions by antibodies against the

cytoplasmic domains of β1, β3, and α5 integrins. Therefore, for studies localizing integrins to focal adhesions, primary antibodies against β1, β3, or α5 integrins were added to fixed permeabilized cells first for 30 minutes at room temperature followed by antibodies against αv and/or vinculin and the incubation continued for another 45 minutes. Cells were then washed and secondary antibodies added as described previously [10]. For studies of focal adhesions using non-permeabilized cells and the β1 integrin activation-dependent antibody 9EG7 and the αv integrin antibody RMV-7 which are both rat monoclonal antibodies, we labeled 9EG7 with FITC using Invitrogen's APEX Alexa Fluor 488 Antibody Labeling kit (#A10468 Molecular probes) and used RMV-7 that had been directly conjugated with biotin (see Table 1) which was detected using Alexa-594 streptavidin (#S11227, Molecular Probes).

Flow cytometry

Wt and sdc1 null CSCs were cultured for three days. Cells were trypsinized using 0.25% Trypsin-EDTA (Gibco #25200-056) for 10 min in a 37°C-7% CO_2 incubator, counted using a Beckman Coulter counter and aliquoted into tubes in volumes corresponding to $(2–4)\times10^5$ cells per tube. Then, cells were centrifuged at 1000 RPM for 5 min, resuspended in blocking buffer (PBS supplemented with 3% BSA) and stained with antibodies against αv or β1 integrins for 30 minutes at 4°C. After staining, cells were washed in blocking buffer and resuspended in 1 ml of PBS; control IgGs were included in each flow cytometry experiment. A FACSCalibur (BD Biosciences) flow cytometer equipped with an air-cooled argon laser and CELLQuest Software was used. The FlowJo 7.6 Software was used to present the data. The results were reproduced with 4 sets of wild type and sdc-1 null CSCs.

Time-lapse studies

Time-lapse imaging experiments were performed as described previously [13]. Cells were seeded onto 24-well plates and either allowed to grow for three days or spread for 2 hours before imaging on an Olympus IX81 research microscope (Olympus America, Melville, NY 11747) equipped with a Proscan motorized stage (Prior Scientific Instruments Ltd., Rockland, MA) and placed in a temperature- and CO_2- controlled chamber (LiveCell Incubation System, Neue Biosciences, Camp Hill PA, 17011). Using relief-contrast optics, images (10×) were acquired per well every 10 min for 16 hr 40 min (100 images). Images were transferred to a workstation equipped with Metamorph image analysis software (Molecular Devices Corporations, Chicago, IL) and velocities of 20 cells per well were calculated using the track cell module. A visual basic program assisted in data analysis. From each cell tracked, an average velocity, net displacement, and total displacement were calculated. In preliminary studies, we have shown that CSC migration rates are independent of cell density when cells were less than 70%–80% confluent (data not shown) and therefore, the studies were performed at these densities unless otherwise noted. Densities are the same for wt and sdc1 null cells in tracking experiments. For experiments involving measurement of cell velocity after replating, wt and sdc1 null cells were initially plated onto 100 mm dishes for harvesting and then onto 24-well plates for tracking which was initiated 2 hours after replating. $MnCl_2$ (1M Stock, Sigma Aldrich #M1787) was added to the media 20 min after cells had been allowed to adhere; cells were then tracked overnight.

Immunoblots

Immunoblots for integrins were performed as described previously [13]. Wt or sdc1 null CSCs were cultured for 3 days. 250 μl of Buffer A [0.1M Tris, pH=8.5, 0.15 M NaCl, 0.5 mM $MgCl_2$, and 0.5% NP-40) was added to each 10 cm culture dish, and the cells were harvested by scraping. Immediately prior to use, 100 μl of 200 mM o-phenathrolin hydrochloride in methanol (Sigma Aldrich #33515), 25 μl Pefabloc SC Plus (Roche # 11 873 601 001), 286μl 7× complete mini protease inhibitor (Roche Complete Mini, # 04 693

124 001) and 20 μl HALT phosphatase inhibitor cocktail (Pierce/ThermoFisher #78420) were added to 2 ml Buffer A. Equal amounts of total protein from each extract were loaded onto 4–20% Tris-glycine gels (Invitrogen # EC6035BOX) and electrophoresis was performed at 140V. The proteins were transferred to PVDF membrane (Millipore # IPVH15150) at 400 mA for 1.5 hour, and the blots blocked in TBS(10X) (Bio-rad # 170–6435) with 0.1% Tween 20 (TBST) and 5% milk overnight at 4°C. Primary and seconday antibodies were added for 1hr each at room temperature (RT), with washes in between. Blots were subjected to ECL reaction (Amersham/GE Healthcare Services # RPN2132), and chemiluminescence was detected using x-ray film. When appropriate, data were quantified using NIH Image software.

Immunoprecipitation

Extracted samples were precleared with Dynabeads (Invitrogen # 10003D) for 15 mins at RT. 3μl of the appropriate primary antibody (Table 1) was added to 30 μl of washed beads and 500μl of Buffer A (see above) and incubated at RT for an hour. The beads were washed 3 times with Buffer A (500 μl). The bead-antibody complex was resuspended in 500ul of Buffer A and 15μg of each cell extract was added and samples incubated overnight at 4°C. After several washes, 30 μl of 1× Lamelli sample buffer (Biorad # 161-0737) with 5% β-mercaptoethanol was added to the beads and samples boiled for 5 minutes. Samples were run, transferred to PVDF membranes and immunoblots performed as described.

Cell adhesion and spreading studies

For cell adhesions studies, CSCs were grown in culture for 3–4 days, trypsinized, and equal numbers of cells were replated and allowed to adhere in the presence or absence of 0.5 mM $MnCl_2$ to uncoated tissue culture plastic, a mixture of fibronectin collagen I (FNCNI; 10 μg/ml human plasma FN (BD Pharmingen), 1% Vitrogen (v:v), 100μg/ml bovine serum albumen in DMEM), or to vitronectin (VN; 10 μg/ml human vitronectin, BD Pharmingen, in DMEM) for 1 hour at 37°C, 7% CO_2. Unattached cells were removed, and adhered cells were fixed and visualized by staining with DAPI and counted. Assays were performed in quadruplicate with three images taken per well and four wells assayed per variable.

For cell spreading studies, day 3–4 cultured wt and sdc1 null CSCs were trypsinized and cells were resuspended in serum-containing media. Equal numbers of cells were allowed to adhere at 37°C, 7% CO_2 for 20 min. Unattached cells were removed, and control or 0.5 mM $MnCl_2$–containing media was added and cells returned to the incubator for a total time of 4 hours. Cells were fixed with 4% paraformaldehyde for 20 minutes at room temperature, permeabilized with 0.1% Triton X-100 for 10 minutes, and stained with an antibody recognizing β-actin. 10× magnification images of β-actin-stained cells were obtained. The areas of no fewer than 80 CSCs were calculated from calibrated images using Image J and the experiments were performed three times.

Quantitative PCR

Quantitiative PCR was performed as described by Cataisson and colleagues [24]. RNA was isolated from cultured corneal stromal cells with TRIZOL (Invitrogen # 15596-026.) following manufacturer's protocol (Invitrogen). For cDNA synthesis, 2 μg of total RNA was reverse transcribed using SuperScript III Reverse Transcriptase (Invitrogen #11752-050). PCR amplifications were performed in a volume of 20 μl. For real-time PCR analysis, the expression levels of sdc1, sdc2, sdc3, and sdc4 cDNA were determined using a Biorad MYiQ iCycler and Gene Expression Macro (version 1.1) from Bio-Rad. cDNA (diluted 1:200 in the final reaction) was measured from triplicate samples using iQ SYBR Green Supermix catalog no.(Bio-Rad #170-8880). The primer sequences for sdc2 and sdc4 were purchased from Qiagen: product numbers QT00144424 for sdc2 and QT00102130 for sdc4.

The primer sequences used for sdc1 were obtained from P.W. Park (Children's Hospital, Boston, MA) and ordered from Invitrogen; the forward sdc1 primer: ATGAGACGCGCGGCGCTCTG and the reverse primer: CTGATTGGCAGTTCCATCCT. The primers used for sdc3 were obtained from Invitrogen; the forward sdc3 primer sequence: ATACTGGAGCGGAAGGAGGT and the reverse primer: TTTCTGGTACGTGACGCTTG. GAPDH primers were purchased from Gene Link (#40-1005-10). Relative standard curves were generated from log input versus the cycle threshold (Ct) and relative levels of cDNAs determined using the comparative Ct method with the cycle threshold difference corrected for GAPDH. Data are presented as fold change in gene expression normalized to GAPDH as described by Onat and colleagues [25]. Experiments were performed in triplicate using cells from three different mouse corneal preparations.

FN Fibrillogenesis Assays

Wild type and sdc1 null CSCs were cultured for five days as described above in the presence of either control media, or media containing $MnCl_2$ or $MgCl_2$. For studies using $MnCl_2$, cells were first allowed to adhere to the coverslips for 2 hours; media was then replaced with media containing $MnCl_2$. To detect endogenous fibrillar FN, CSCs were fixed in 4% paraformaldehyde for 15 minutes, permeabilized with 0.1% Triton X100 for 10 minutes, immunostained with a polyclonal antibody recognizing FN (courtesy of Dr. K.M. Yamada), and counterstained with DAPI to show cell nuclei. Cells were imaged on an inverted fluorescence microscope (Cell Observer Z1, Carl Zeiss) with a CCD camera (Axiocam MRm, Carl Zeiss). Total pixel intensity for endogenous FN was quantified using MetaVue (Version 6.2r6, Molecular Devices), and normalized to total pixel intensity in the UV channel for a minimum of five images per condition.

To identify incorporation of exogenously added FN into a fibrillar matrix, purified human plasma FN [26] that was labeled with $Alexa^{647}$ [27] was added to CSC cell cultures at 0.02 μg/μL. After 72 hours in culture, cells were fixed as described (but not permeabilized), and co-stained with an antibody recognizing FN.

Sodium deoxycholate (DOC) extractions were performed as reported previously [28], except that cells were collected into 2% DOC extraction with a mini protease inhibitor tablet (Roche) and analyzed by Western analysis, as described [29]. Briefly, 3 mg of protein was loaded per well on a 1-mm NuPAGER 4–12% Bis-Tris gel, electrophoresed, and transferred to a PVDF membrane using the Invitrogen XCell Surelock system (Invitrogen). Chemiluminescent blots were imaged using x-ray film (ECL Hyperfilm, Amersham) and bands quantified using Quantity One (Version 4.6.1, BioRad) with normalization to GAPDH. Each experiment was repeated at least three times, but a single representative blot and its quantification are shown for each DOC assay.

Statistics

Data were subjected to statistical analyses using either InStat or Prism software (Graphpad Software, Inc.). Unless otherwise indicated, the differences between groups were evaluated by ANOVA (Analysis of Variance) and post tests as recommended by statistics software to evaluate differences between specific data points. For cell spreading and time-lapse imaging studies, data were considered significant for p values less than 0.05 for ANOVA tests; for studies of FN fibrillogenesis, data were considered significant for p values of less than or equal to 0.001 for the ANOVA tests. Bar graphs were generated using means and standard error of the mean (SEM) values.

Results

Sdc1 is observed in the posterior mouse corneal stroma within 24 hours after wounding and in a subpopulation of cultured wt CSCs

BALB/c mouse corneas were wounded by manual debridement and their corneas were used to assess the localization of sdc1 in the corneal stroma in response to injury. While most CSCs do not express sdc1, some sdc1-positive cells are found in the posterior stroma at two and three days after injury (Figure 1A). FN expression increases in the posterior corneal stroma after wounding. While a few cells in the posterior stroma do express FN, sdc1 and FN do not co-localize. Unwounded corneas do not express detectable FN or sdc1 in the stroma (data not shown).

To study the role of sdc1 in the corneal stroma in an in vitro model, mouse corneal stromal cells (CSCs) were isolated from the corneas of wt and sdc1 null mice and maintained in media supplemented with serum. CSCs were stained for the presence of sdc1 and vimentin at two and five days after being placed into primary cell culture (Figure 1B). All of the primary cells obtained from the wt and sdc1 null adult mouse corneas were vimentin positive and since corneal epithelial and endothelial cells do not express vimentin, these cells can be classified as CSCs. A subpopulation of the wt CSCs were positive for sdc1 at days two and five. The sdc1 null CSCs were well spread and their vimentin-positive intermediate filaments showed a similar localization to those observed in the wt cells. Additional immunostaining indicated that wt and sdc1 null CSCs were positive for both nestin and αSMA within two days of being placed in primary culture, but there were no differences between these genotypes in the distribution of either cytoskeletal protein (data not shown).

We also assessed the expression of sdc family members in wt and sdc1 null CSCs using QPCR. While sdc1 is expressed by wt CSCs and not sdc1 null CSCs, both genotypes expressed sdc2, sdc4, and sdc3 mRNAs in decreasing amounts (Figure 1C). Sdc3 expression in CSCs, like that of nestin, reflects their neural crest origin. While there was a trend for the sdc1 null CSCs to express more sdc2, 3, and 4 mRNAs than the wt cells, the difference was not significant (Fig 1C). Thus, we find no evidence for compensation by other sdc homologs in sdc1 null cells at the level of mRNA expression.

CSCs derived from sdc1 null mice migrate faster than those from wt mice

Using time-lapse microscopy, we next assessed the migration rates of the CSCs in vitro in media containing 10% serum. Representative tracks obtained from 10 wt and sdc1 null cells maintained in 10% serum-containing media are shown in Figure 2A. The red tracks indicate the paths taken by the cells during the time in which 100 images were taken. The tracks from the sdc1 null cells are longer than those from the wt cells (Fig. 2A). Quantification of data from 90 cells tracked for each variable are shown in Figure 2B along with similar data from cells grown in defined keratocyte media, which maintains cells in their quiescent state. Sdc1 null cells maintained in 10% serum migrated significantly faster than wt cells; both genotypes responded to media lacking serum by reducing their migration rate; under quiescent conditions, there is no difference in the rate of migration between these two genotypes of CSCs.

There is no difference in the total amount of several different integrin α and β chains expressed by wt and sdc1 null CSCs or in the surface expression of αv-containing and β1-containing integrins

To determine whether differences in integrin expression are detectable in sdc1 null and wt CSCs, we examined the expression of several integrin α (α5, α7, αv) and β (β1, β3, β5)

chains by immunoblotting; a minimum of 4 different preparations of CSCs were used for each protein. Immunoblot data are shown in Figure 2C for CSCs extracted using a mild 0.5% NP40-containing extraction buffer; graphs represent data following normalization for expression of β-actin. There was a trend for αv and β1 integrin and αSMA to be elevated in sdc1 null CSCs but these differences were not statistically significant. We repeated these immunoblot studies using harsher cell extraction conditions and again saw no significant difference in αv, β1, and β3 integrin expression between genotypes (data not shown). We also quantified the expression of αSMA in NP40 extracts, as an indicator of conversion of CSCs into myofibroblasts, and found it slightly elevated in sdc1 null CSCs but the difference was not statistically significant.

To determine whether there were also similar levels of integrins on the cell surface, we performed flow cytometry studies. Due to limited availability of antibodies against the extracellular domains of mouse integrins, we evaluated αv and β1 integrins by flow cytometry; data are presented in Figure 2D for αv and β1. Surface expression levels of αv and β1 integrins were similar. To confirm the flow cytometry results, we also performed surface biotinylation using procedures we have used previously to assess surface integrin expression [14, 15] and found similar surface expression of αv and β1 integrins using that technique (data not shown).

αv and β1 integrins are found within CSC focal adhesions, and αvβ1 heterodimers are present on both wt and sdc1 null CSCs

CSCs adhere to substrates via integrin-containing attachments that transduce signals to the cytoskeleton and organize stress fibers into focal adhesions (FAs) as the cells spread. Some of the FAs convert into fibrillar adhesions (FBAs). FAs and FBAs are highly dynamic and at any given time, adherent cells have a mixture of both types of adhesion complexes [30]. While FAs mediate tractional force generation and cell migration, FBAs are the sites of assembly of FN fibrils. In fibroblasts, both αvβ3 and α5β1 integrins have been shown to be present in FAs. FBAs have been reported to be enriched in α5β1 but not αvβ3 [29]; however, FBAs containing both α5β1 and αvβ1 have not been reported. We examined the adhesions formed by wt and sdc10 null cells and evaluated the localization of β1 and αv integrins along with vinculin (Figure 3A) and α5 and β3 integrins along with αv integrin (Figure 3B). The α5 and β1 antibodies used for the studies shown in Figure 3 recognize the cytoplasmic domains of the proteins whereas the αv and β3 antibodies recognize extracellular epitopes. Therefore, the cells were permeabilized to allow penetration of the cytoplasmic domain antibodies and the vinculin antibody in Figure 3A. These data represent the localization of both active and inactive and surface and intracellular pools of integrins. Data showing the localization of αv and β1 at sites of focal adhesions in CSCs are presented in Figure 3A. The average fluorescence intensity of vinculin within FAs located at cell peripheries and the ratios of αv or β1 integrin fluorescence intensity at the cell periphery in comparison with vinculin are presented beneath the images in Figure 3A. Both β1 and αv integrins localized to FAs in wt and sdc1 null cells, and wt adhesions contain significantly more αv integrin and significantly less β1 integrin compared to sdc1 null cells.

The major β1 family integrin expressed on CSCs has been reported to be α5β1 whereas the major αv-containing integrin is reported to be αvβ3. We immunostained permeabilized CSCs to examine the localization of αv, α5, and β3 integrins and found low levels of α5 and β3 integrin within the αv-positive FAs seen in wt and sdc1 null CSCs (Figure 3B). These data make it unlikely that α5β1 and αvβ3 heterodimers are the major integrins found within the β1- and αv-positive focal adhesions.

The co-localization of β1 and αv at focal adhesions suggests that these two integrin α and β chains may form heterodimers with one another. To investigate this possibility, we

immunoprecipitated equal amounts of wt and sdc1 null CSC extracts with antibodies against β1, β3, α5, and αv integrins and blotted the immunoprecipitates with antibodies against αv or β1 integrin. If β1 forms heterodimers with αv, we expect to see αv in the β1 immunoprecipitates and β1 in the αv immunoprecipitates. Integrins cluster within FAs and FBAs and have been shown to co-immunoprecipitate with one another making it difficult to determine whether αvβ1 heterodimers exist or if, for example, α5β1 and αvβ3 co-immunoprecipitate with one another. We reason that if there is co-immunoprecipitation of multiple integrin heterodimers with one another, we would detect those events with the α5 and β3 immunoprecipitates since the α5 immunoprecipitation should detect β1 but not αv and the β3 immunoprecipitation should detect αv but not β1.

The results of the immunoprecipitation studies are presented in Figure 3C. When we blot for αv, we observe the most αv in the αv and β3 immunoprecipitations as expected but none in the α5 immunoprecipitation showing that there is no evidence for co-immunoprecipitation of αv-containing heterodimers with α5β1 integrin in CSC extracts. We also see a clear band for αv in the β1 immunoprecipitate indicating the presence of αvβ1 heterodimers. Replicate blots probed to detect β1 integrin confirm the specificity of the immunoprecipitations and verify the presence of β1 in the αv immunoprecipitates (data not shown). We used similar amounts of wt and CSC extracts for these immunoprecipitates and detected similar amounts of αv in the wt and sdc1 null β1 immunoprecipitates. While these results suggest that both wt and sdc1 null CSCs have similar levels of αvβ1, they can not be considered to be quantitative due to variability in both the efficiency of extraction and immunoprecipitation of proteins localized within focal and fibrillar adhesions.

Activation of integrins by cations using $MnCl_2$ alters cell adhesion, spreading, and migration in sdc1 null cells

Thus far we have shown that integrin expression is similar in wt and sdc1 null CSCs, despite the fact that the sdc1 null CSCs migrate 1.8 times faster than wt cells. We next assessed the ability of wt and sdc1 null CSCs to adhere, spread, and migrate in response to replating onto low concentrations of integrin ligands on uncoated tissue culture dishes or onto surfaces coated with high concentrations of the β1 integrin substrate fibronectin/collagen I (FNCN1) or the αv integrin ligand vitronectin (VN) and in response to treatment with the cationic integrin activator, $MnCl_2$. Data are presented in Figure 4A–D.

Adhesion Studies—Equal numbers of wt and sdc1 null CSCs were allowed to adhere to uncoated, FNCNI, or VN coated tissue culture wells for 1 hour in the presence or absence of 0.5 mM $MnCl_2$. $MnCl_2$ has been shown to convert integrins from their inactive to active conformations [31, 32]. Results in Figure 4A show that wt and sdc1 null cells adhere similarly to each of the ligands tested but that both genotypes prefer to adhere to FNCN1 compared to VN. $MnCl_2$ treatment increased adhesion for both genotypes of cells adhering to low concentrations of integrin ligands on the uncoated wells but had no impact on adhesion to FNCN1 or VN. These data show that $MnCl_2$-mediated integrin activation increases CSC adhesion only when integrin ligands are present at low concentrations. When integrin ligands are present at high concentrations, the integrin that mediate adhesion become activated via outside-in signaling, and $MnCl_2$ does not have any added affect on cell adhesion.

Cell Spreading Studies—Spreading studies were performed by allowing CSCs to adhere to the indicated surface without cation treatment for 20 min; after unattached cells were removed, cells were either treated with cell culture media alone or media supplemented with 0.05 mM $MnCl_2$. If all of the integrins on cell surfaces are active, the ratio of the mean spread area after $MnCl_2$ treatment/the mean spread area of control cells, a value we call the

$MnCl_2$-induced integrin activation index, would be 1.0. Cells with integrins on their surface in the inactive state will respond to $MnCl_2$ and spread more, and have higher $MnCl_2$-induced integrin activation indices. Differences in $MnCl_2$-induced spreading on substrates that engage primarily β1 (FNCN1), αv (VN), or both (uncoated tissue culture plastic) classes of integrins provide a measure of β1 and αv integrin activity during spreading on these substrates. The spread areas were measured for a minimum of 84 cells for each variable tested from 3 independent CSC preparations on all three substrates with and without $MnCl_2$ treatment.

Wt and sdc1 null CSCs both spread more on FNCN1 compared to uncoated and VN coated surfaces and there were no differences between genotypes as shown in Figure 4B. However, when we examined cell spreading in the presence of $MnCl_2$, sdc1 null cells were significantly more spread compared to wt cells on all three surfaces tested, with VN-adhered sdc1 null CSCs showing the most pronounced increase in cell spreading after $MnCl_2$-treatment. $MnCl_2$-induced integrin activation indices calculated from these experiments are shown below the graph for the spreading data in Figure 4B. The largest activation index for both genotypes is obtained for cells plated onto VN where it is 1.8 for wt cells and 2.7 for sdc1 null cells in the presence of $MnCl_2$.

We also immunostained cells used for cell spreading assays to reveal the state of organization of the actin cytoskeleton and their focal adhesions after replating. For these analyses, we used cells that had been allowed to spread in the presence of $MnCl_2$ for 4 hours after adhesion to uncoated surfaces. Shown in Figure 4C, the actin cytoskeleton in control wt cells is poorly organized with few filaments present by 4 hours and becomes better organized in the presence of $MnCl_2$; discrete vinculin containing focal adhesions are rare. In sdc1 null cells, the actin cytoskeleton is better organized and vinculin containing focal adhesions are present without $MnCl_2$ and with $MnCl_2$, numerous prominent focal adhesions are seen. These results show that reassembly of focal adhesions occurs more rapidly in sdc1 null cells compared to wt cells and is enhanced by $MnCl_2$ treatment.

Cell Migration Studies—If integrins on the surface of sdc1 null cells are less active than those on wt cells, then replating the cells onto FNCN1 or VN should partially or completely revert the cell migration differences seen in sdc1 null cells. CSCs were replated onto uncoated, FNCN1-, or VN-coated surfaces and, after 2 hours, were allowed to migrate in the absence or presence of $MnCl_2$ and analyzed using time-lapse microscopy. Quantification of cell velocities is shown in Figure 4D. Sdc1 null cells migrated 1.8, 1.4, and 1.3 fold faster than wt cells on uncoated, FNCN1-, and VN-coated surfaces, respectively. As integrins are activated by adhesion to high concentrations of both integrin ligands, the migration rate of both wt and sdc1 null cells decreases and the decrease is more dramatic for sdc1 null cells.

The non-specific activation of integrins by $MnCl_2$ would also be predicted to reduce wt and sdc1 null cell migration rates with the impact more pronounced on sdc1 null cells. In fact, $MnCl_2$ reduced the migration rate of wt CSCs on uncoated and FNCN1 coated surfaces but had no impact on wt cells migrating on VN coated surfaces. For sdc1 null CSCs, $MnCl_2$ eliminates differences in velocity on all three substrates tested.

The rat monoclonal antibody 9EG7 preferentially binds active, ligand bound β1 integrin on cell surfaces [33]. The hamster monoclonal antibody Ha2/5 also recognizes the β1 integrin extracellular domain, but does not bind to ligand-bound β1 integrin [34]. No antibodies are available that detect surface β1 integrin in mouse cells and are not sensitive to the activation state of the integrin. Data for the immunostaining of non-permeabilized wt and sdc1 null CSCs with and without $MnCl_2$ treatment with these antibodies are presented in Figure 5A along with quantification of the ratios of the fluorescence intensity obtained for the activated

integrin epitope relative to that obtained using Ha2/5. We determined these ratios for sites adjacent to the cell nucleus near cell centers as well as at the periphery of each cell to allow us to determine whether integrin activation at sites where FBAs form could be differentiated from those where FAs assemble. In control wt and sdc1 null cells, there was less activated β1 integrin present within clusters at both the center and periphery of the CSCs but the difference was greater for the central clusters compared to the peripheral clusters. $MnCl_2$ treatment eliminated the difference detected in β1 integrin activation in wt and sdc1 null CSCs.

Next we looked at whether we could observe evidence for active αvβ1 within FAs and FBAs on the surfaces of wt and sdc1 null cells by immunostaining non-permeabilized CSCs with antibodies 9EG7 and with RMV-7, which detects αv integrin. Since both 9EG7 and RMV-7 are rat monoclonal antibodies, for these studies we used Alexa-488-conjugated 9EG7 and biotinylated RMV-7 and visualized the biotinylated αv antibody using Alexa-594 conjugated streptavidin. Data presented in Figure 5B shows that in untreated wt cells, FAs at the cell periphery co-label with both the 9EG7 and αv antibodies (arrows) but there are also 9EG7-positive adhesions that do not show αv integrin (arrowheads). $MnCl_2$ increases the numbers of double positive 9EG7 and αv-positive adhesions; yet, after $MnCl_2$ treatment not all adhesions contain both integrins. Prior to treatment, sdc1 null cells had fewer peripheral FAs positive for both integrins and after $MnCl_2$ treatment, there was an increase in both double positive and singly αv-positive focal adhesions in sdc1 null CSCs. The fluorescence intensity ratios comparing 9EG7 to RMV-7 were calculated for central FBAs and for peripheral FAs and are presented in Figure 5B for both the untreated cells and for cells treated with $MnCl_2$. The fluorescence intensity ratios comparing activated β1 integrin to αv integrin are significantly higher for wt cells except for the central adhesions after $MnCl_2$ treatment where the ratio of activated β1 integrin to αv integrin is the same for wt and sdc1 null cells. These studies show that prior to integrin activation, there are more ligand bound αvβ1-positive FBAs and FAs in the wt cells compared to sdc1 null cells; after activation, wt cells still have higher ratios of 9EG7 to RMV7 in the peripheral adhesions.

Focal adhesions express β1 and αv integrins, as detected by immunostaining with a cytoplasmic domain antibody against β1 integrin and with the αv antibody RMV-7; the smaller sdc1 null FAs shown in Figure 3 had less αv integrin but more total β1 integrin present. The data presented in Figure 5A and B show only surface integrins. These data demonstrate that the β1 integrin present within in the peripheral FAs of sdc1 null cells is less active as determined by 9EG7 staining and confirm that these FAs have less αv integrin. In sdc1 null cells, $MnCl_2$ activation increased β1 integrin activity within peripheral FAs but differences in the ratio of activated β1 integrin to αv integrin persist after treatment. We conclude that the most of the β1 integrin present in the sdc1 null CSC FAs prior to $MnCl_2$ treatment is not ligand bound and therefore, is not fully active.

Sdc1 regulates FN fibrillogenesis in wt and sdc1 null CSCs

It has been previously demonstrated that α5β1 integrin activity regulates the formation of FN fibrils at cell surfaces [35], and much research has been conducted to demonstrate the mechanisms by which integrin-FN interaction induces the self-assembly of FN monomers [36]. An important finding is that sdc4 acts as a co-receptor with α5β1 integrin to affect cell-mediated FN fibrillogenesis [37, 38]. Since sdc1 null CSCs have fewer active β1 integrin clusters within FBAs as shown in Figure 5A, we hypothesize that assembly of FN on cell surfaces may be altered.

We first used immunofluorescence to assess the localization of FN in cells after 5 days in culture; we observed reduced amounts of assembled FN fibrils on the surface of the sdc1 null CSCs (Figure 6A). Since FN is present in both intracellular and extracellular pools we

questioned whether there was a difference in FN expression, secretion, or assembly at the cell surface. When FN is incorporated into fibrils in vitro, it becomes insoluble in deoxycholate (DOC); FN monomers and dimers, both intracellular and at the cell surface, are soluble in DOC [27]. When CSCs were fractionated using DOC, equal amounts of FN were detected in the soluble and insoluble fractions in wt cells but, by contrast, in the sdc1 null cells, most of the FN was detected in the soluble fraction (Figure 6B) confirming that less FN was incorporated into fibrils in the null cells. When cells were extracted with a buffer that solubilizes all of the FN, there was no difference in the total amount of FN expressed by both wt and sdc1 null cells (Figure 6B).

Fluorescently-tagged soluble FN can be directly added to the media of cells in culture and the assembly of labeled FN into FN fibrils can be assessed and compared to that of unlabeled FN fibrils. In the presence of fluorescently labeled FN, there were also fewer fluorescently tagged FN-fibrils assembled on sdc1 null CSCs compared to the wt cells (Figure 6C). Therefore, the reduced FN fibrils that accumulate around sdc1 null cells, shown in Figure 6A, is not caused by differences in the secretion of FN molecules. Taken together with the results shown in Figure 5 demonstrating that the β1 integrins are less active in sdc1 null cells, these data indicate that the reduced levels of FN fibers is a function of the reduced activity of the integrins on the surface of the sdc1 null CSCs.

We have shown that sdc1 null cells migrate faster than wt cells and that $MnCl_2$ treatment can revert the migration phenotype by activating β1 integrins. We next questioned whether $MnCl_2$ could also affect FN assembly in these cells. When we assessed FN fibrillogenesis in the presence of increasing concentrations of $MnCl_2$, we found that the reduced FN-fibrillogenesis phenotype in the sdc1 null CSCs could be reverted (Figure 7A and B). $MnCl_2$ enhanced the formation of DOC insoluble FN in both wt and sdc1 null cells (Figure 7C) and also increased the assembly of unlabeled and fluorescently tagged FN into FN fibrils (Figure 7D).

Dermal Fibroblasts lacking sdc1 assemble FN matrices

CSCs are derived from neural crest cells, whereas dermal fibroblasts (DFs) are derived from mesenchymal cells. Both cell types are activated during wound healing to become myofibroblasts and have important functions in wound healing. Primary DFs derived from sdc1 null mice migrate faster and have reduced αv integrin functions despite having increased levels of αv integrin on their surface [13], but have not been evaluated for FN fibrillogenesis. To determine whether sdc1 null DFs show similar differences to CSCs in FN assembly, we performed FN assembly studies using primary DFs, as shown in Figure 8. Both primary wt and sdc1 null dermal fibroblasts assemble FN fibrils but sdc1 null cells assemble more FN fibrils in comparison to wt DFs both by immunostaining and biochemically. Immunoblots to assess total and DOC soluble and insoluble FN showed that primary sdc1 null DFs express elevated levels of total and DOC-insoluble FN. To confirm that these differences were not due to differences between primary cells and later passage cells, we repeated staining studies using 4^{th} passage DFs and obtained similar results to those seen for primary cells (data not shown). Therefore, the reduced FN fibril assembly observed in sdc null CSCs is tissue-specific. We conclude that sdc1 can regulate FN fibrillogenesis in cells derived from both corneal and dermal tissues but whether fibrillogenesis increases or decreases when sdc1 is lacking is cell type specific.

Discussion

In this study we show for the first time that lack of syndecan-1 alters both cell migration rates and FN fibrillogenesis in cells derived from the corneal stroma. CSCs derived from sdc1 null mice migrate faster and assemble FN fibrils at their cell surface poorly. The total

and surface expression of β1 and αv integrins, as determined by immunoblots and flow cytometry, respectively, are similar for both genotypes and we demonstrate for the first time the presence of αvβ1 on the surface of these CSCs. Cell adhesion, spreading, and migration studies show that the loss of sdc1 alters the activity of integrins that bind FN and CN as well as VN-binding integrins. These differences lead to smaller focal adhesions that permit faster migration but reduce FN fibrillogenesis. Unlike sdc1 null CSCs, sdc1 null DFs secrete more total FN and assemble more insoluble FN fibrils despite migrating faster than wt DFs. We had previously reported that the FAs of sdc1 null DFs appear larger than those of wt DFs [13]; however, those differences were not quantified. The sdc1 null cells are more migratory and migrating cells have polarized morphologies with larger FAs at their trailing edge than their leading edge. In the quantification we did on the CSCs, we took care to use the line tool to highlight several regions at the periphery of several cells to make sure that we did not bias the data towards migrating cells. Taken together, our results demonstrate a role for sdc1 in the formation of FN fibrils in CSCs and DFs via its ability to regulate integrin activation.

When we examined localization of αv and β1 integrin and the cytoplasmic FA molecule vinculin within FAs on sdc1 null CSCs after permeabilization to allow binding of antibodies to vinculin, we observed smaller FA on sdc1 null cells than on wt cells. Smaller FAs can result from decreased FA assembly or increased disassembly. The results of our cell spreading studies demonstrate that FA assembly is enhanced in sdc1 null cells and because these cells migrate faster than wt cells, their FAs must disassemble faster. When we studied the localization and expression of an activation dependent β1 integrin epitope [33] on non-permeabilized cells, we found that FAs and FBAs in wt cells contained more activated β1 integrin than those on sdc1 null cells. FAs and FBAs on sdc1 null cells are also smaller and contain less αv integrin than those of wt cells. We conclude that the FAs of sdc1 null CSCs are less efficient at converting to FBAs and organizing and assembling FN fibrils. The reduced accumulation of active β1 integrin at FAs, while permissive for rapid FA turnover and faster migration, reduces FN fibrillogenesis.

Sorting out the adhesion and migration properties of cells is complicated by the large number of distinct integrin αβ heterodimers that are present. αv integrin can form heterodimers with β1, β3, β5, β6, and β8 subunits. Studies on αv integrins are often conducted using β subunit-specific antibodies which allow investigators to specifically probe contributions of αvβ3 and αvβ5 for example but do not take into account the possibility that αvβ1 might also be present. Like αv, the integrin β1 subunit can associate with numerous different α chains as well as with αv. On finding that sdc1 null cells had a FN-fibrillogenesis phenotype, we extended our immunoblot survey of expression of integrin α chains in wt and sdc1 null CSCs to all of those known to be involved in mediating FN-binding including α4, α8, and α9 integrins. We found no significant differences in the total expression of these integrins but we can not rule out differences in their cell surface expression (data not shown).

Considering data from others showing that in wt cells expressing sdc1, the proteoglycan binds to αvβ3 and αvβ5 integrins and modulates their function [39, 40] and our data showing reduced integrin functions on CSCs lacking sdc1, we hypothesize that in wt cells, sdc1 bound to αv-containing integrins enhances their function. A model presented schematically in Figure 9 A and B shows the impact of the loss of sdc1 on integrin activation and functions at the molecular (A) and cellular (B) levels. In wt cells, sdc1 interacts with newly synthesized integrins; data implicate that this interaction occurs via the β3 and β5 chains and does not require the presence of the heparan sulfate side chains of sdc1 [40]. Integrins are synthesized as inactive molecules. Full activation occurs in stages starting from the inactive state with ectodomain head groups in a folded conformation that can not bind ligands and with cytoplasmic tails closely overlapping one another to prevent the binding of talin,

vinculin and other focal adhesion components. During activation, the conformation of integrin heterodimers changes and the molecules go through an intermediate stage, also termed a primed stage, to eventually become active with their α and β head domains extended and their cytoplasmic domains pushed apart to permit optimal assembly of focal adhesion and adaptor proteins [41].

We hypothesize that in wt cells integrins proceed from their inactive to active states via the primed state, that most integrins are either inactive or active on wt cells, and the integrins that accumulate in FAs and FBAs are mostly in their active state. In sdc1 null cells, our data show that integrins accumulate within FAs. To become clustered within focal adhesions, inactive sdc1 null integrins must change their conformation--either their cytoplasmic tails must move apart as in inside-out signaling or their head domains must open-up to expose their ligand binding site as during out-side in signaling. The 9EG7 antibody binds preferentially to the activated ligand-bound form of β1 integrin and its expression remains low in sdc1 null FAs and FBAs. Our data suggests that the cytoplasmic tails of the integrins in sdc1 null FAs and FBAs must have moved apart sufficiently to permit talin and vinculin to accumulate within adhesion sites but this primed conformation does not proceed to full activation and unfolding of the head domains with the same efficiency in sdc1 null cells as it does in wt cells.

If this model is correct, it predicts that integrins on sdc1 null cells would be less capable of regulating events controlled by inside-out integrin signaling. Cell adhesion to high concentrations of FNCNI-containing matrices was not impacted by the loss of sdc1. This indicates that integrins on sdc1 null cells are capable of responding to surface-bound matrix molecules at high concentration. Yet, assembly of FN fibrils at the cell surface is defective in sdc1 null CSCs and FN molecules in solution do not induce activation of integrins with the same efficiency as in wt cells indicating that there are also differences in outside-in signaling in cells lacking sdc1.

FN fibrillogenesis requires the presence of functional integrins on the cell surface; the best studied of these is α5β1. During the maturation of FAs into FBAs, studies have shown that αvβ3 remains within FAs and α5β1 is recruited into newly forming FBAs [35]. While the detailed mechanism of how these events are regulated is not totally clear, proteins that associate with the β1 subunit are required for the formation of mature FBAs [42]. Our results indicate that the ratio of activated β1 integrin to αv integrin is greater in FBAs than in FAs in wt cells, and yet the overall amount of activated β1 integrin is similar in wt FBAs and FAs. Therefore, in wt CSCs αvβ1 appears to be recruited into FBAs along with α5β1. Sdc1 null cells have less activated αvβ1 in their FBAs and form FN fibrils less efficiency. Whether the reduced formation of FN fibrils is a result of reduced activation of αvβ1 at these sites remains to be determined.

The fact that the sdc1 null CSCs and dermal fibroblasts regulate FN assembly differently is intriguing, and it will be important to determine exactly why and how these differences arise. Studies using sdc1 ectodomain derived peptides hold promise to help sort out these events. Data from Beauvais and colleagues [40] show that sdc1 peptides can inhibit integrin activity in cancer cells. If sdc1 peptides regulate FN fibrillogenesis, a new tool for the treatment of fibrosis could be available. While regulation of FN fibrillogenesis is important during wound healing in the skin, it is even more critical in vivo in the cornea. The primary function of the CSCs in vivo is to regulate the assembly of collagen fibrils within the corneal stroma. Collagen assembly has an absolute requirement for a preformed FN matrix both during development and wound healing [3]. The integrin-mediated cell signaling events that permit the exquisite regulation of tissue organization required to create and maintain a clear corneal stroma in vivo have been shown to require fibronectin and integrins, as well as

several collagen fibril nucleators, and several fibril diameter regulators which include proteoglycans like lumican and decorin [3, 43, 44]. Since sdc1 regulates FN fibril formation, our results suggest that sdc1 should also be considered to be one of the regulators of corneal stromal collagen formation.

When the cornea is wounded, scarring takes place when wound-activated CSCs attempt to recreate the ordered environment that surrounded them before wounding by degrading some collagen fibrils and re-synthesizing others. Corneal scarring is a major cause of blindness worldwide as consequence of fungal and parasitic infections [45]. A better understanding of how this process is regulated by syndecans and integrins within the cornea and skin will provide better tools for developing treatments for diseases of corneal scarring and for fibrotic diseases of various organs.

Acknowledgments

The authors would like to acknowledge Kenneth M. Yamada for the anti-fibronectin antibody, Christophe Cataisson for help with the QPCR, and Alan Rapraeger, Deanne Mosher, Donna Pesciotta Peters, Pwong Woo Park, and James D. Zieske for helpful discussions. Funding was provided by NIH RO1 EY08512 to MAS and DE019244401, DE019197, and RC1DE020402 to ML.

REFERENCES

1. Kao WW, Liu CY. Roles of lumican and keratocan on corneal transparency. Glycoconj. J. 2002; 19:275–285. [PubMed: 12975606]
2. Carlson EC, Liu CY, Chikama T, Hayashi Y, Kao CW, Birk DE, Funderburgh JL, Jester JV, Kao WW. Keratocan, a cornea-specific keratan sulfate proteoglycan, is regulated by lumican. J. Biol. Chem. 2005; 280:25541–25547. [PubMed: 15849191]
3. Kadler KE, Hill A, Canty-Laird EG. Collagen fibrillogenesis: fibronectin, integrins, and minor collagens as organizers and nucleators. Curr. Opin. Cell Biol. 2008; 20:495–501. [PubMed: 18640274]
4. Chen LD, Hazlett LD. Perlecan in the basement membrane of corneal epithelium serves as a site for P. aeruginosa binding. Curr. Eye Res. 2000; 20:260–267. [PubMed: 10806439]
5. Stepp MA, Gibson HE, Gala PH, Sta.Iglesia DD, Pajoohesh-Ganji A, Pal-Ghosh S, Brown M, Aquino C, Schwartz AM, Goldberger O, Hinkes MT, Bernfield M. Defects in keratinocyte activation during wound healing in the syndecan-1-deficient mouse. J. Cell Sci. 2002; 115:4517–4531. [PubMed: 12414997]
6. Park PW, Reizes O, Bernfield M. Cell surface heparan sulfate proteoglycans: selective regulators of ligand-receptor encounters. J. Biol. Chem. 2000; 275:29923–29926. [PubMed: 10931855]
7. Perrimon N, Bernfield M. Cellular functions of proteoglycans--an overview. Semin Cell Dev Biol. 2001; 12:65–67. [PubMed: 11292371]
8. Hayashida K, Stahl PD, Park PW. Syndecan-1 ectodomain shedding is regulated by the small GTPase Rab5. J Biol. Chem. 2008; 283:35435–35444. [PubMed: 18957427]
9. Bass MD, Morgan MR, Humphries MJ. Syndecans shed their reputation as inert molecules. Sci Signal. 2009; 2:pe18. [PubMed: 19336838]
11. Stepp MA, Liu Y, Pal-Ghosh S, Jurjus RA, Tadvalkar G, Sekaran A, Losicco K, Jiang L, Larsen M, Li L, Yuspa SH. Reduced migration, altered matrix and enhanced TGFβ1 signaling are signatures of mouse keratinocytes lacking Sdc1. J. Cell Sci. 2007; 120:2851–2863. [PubMed: 17666434]
10. Stepp MA, Pal-Ghosh S, Tadvalkar G, Rajjoub L, Jurjus RA, Gerdes M, Ryscavage A, Cataisson C, Shukla A, Yuspa SH. Loss of syndecan-1 is associated with malignant conversion in skin carcinogenesis. Mol. Carcinog. 2010; 49:363–373. [PubMed: 20082322]
12. Pal-Ghosh S, Tadvalkar G, Jurjus RA, Zieske JD, Stepp MA. BALB/c and C57BL6 mouse strains vary in their ability to heal corneal epithelial debridement wounds. Exp. Eye Res. 2008; 87:478–486. [PubMed: 18809399]

13. Jurjus RA, Liu Y, Pal-Ghosh S, Tadvalkar G, Stepp MA. Primary dermal fibroblasts derived from sdc-1 deficient mice migrate faster and have altered αv integrin function. Wound Repair Regen. 2008; 16:649–660. [PubMed: 19128260]
14. Hay ED. Development of the vertebrate cornea. Int. Rev. Cytol. 1979; 63:263–322. [PubMed: 395131]
15. Cvekl A, Tamm ER. Anterior eye development and ocular mesenchyme: new insights from mouse models and human diseases. Bioessays. 2004; 26:374–386. [PubMed: 15057935]
16. Jester JV, Huang J, Barry-Lane PA, Kao WW, Petroll WM, Cavanagh HD. TGFβ-mediated corneal myofibroblast differentiation requires actin and fibronectin assembly. Invest. Ophthalmol. Vis. Sci. 1999; 40:1959–1967. [PubMed: 10440249]
17. Masur SK, Conors RJ Jr, Cheung JK, Antohi S. Matrix adhesion characteristics of corneal myofibroblasts. Invest. Ophthalmol. Vis. Sci. 1999; 40:904–910. [PubMed: 10102287]
18. Bernstein AM, Twining SS, Warejcka DJ, Tall E, Masur SK. Urokinase receptor cleavage: a crucial step in fibroblast-to-myofibroblast differentiation. Mol. Biol. Cell. 2007; 18:2716–2727. [PubMed: 17507651]
19. Wilson SE, Liu JJ, Mohan RR. Stromal-epithelial interactions in the cornea. Prog. Retin. Eye Res. 1999; 18:293–309. [PubMed: 10192515]
20. Stepp MA, Spurr-Michaud S, Tisdale A, Elwell J, Gipson IK. α6β4 integrin heterodimer is a component of hemidesmosomes. Proc. Natl. Acad. Sci. U. S. A. 1990; 87:8970–8974. [PubMed: 2247472]
21. Stepp MA. α9 and β8 integrin expression correlates with the merger of the developing mouse eyelids. Dev. Dyn. 1999; 214:216–228. [PubMed: 10090148]
22. Marcantonio EE, Hynes RO. Antibodies to the conserved cytoplasmic domain of the integrin β1 subunit react with proteins in vertebrates, invertebrates, and fungi. J. Cell Biol. 1988 May. 106:1765–1772. 1988. [PubMed: 3131349]
23. Sta.Iglesia DD, Gala PH, Qiu T, Stepp MA. Integrin expression during epithelial migration and restratification in the tenascin-C deficient mouse cornea. J. Histochem. Cytochem. 2000; 48:363–376. [PubMed: 10681390]
24. Cataisson C, Pearson AJ, Tsien MZ, Mascia F, Gao JL, Pastore S, Yuspa SH. CXCR2 ligands and G-CSF mediate PKCα-induced intraepidermal inflammation. J. Clin. Invest. 2006; 116:2757–2766. [PubMed: 16964312]
25. Onat D, Jelic S, Schmidt AM, Pile-Spellman J, Homma S, Padeletti M, Jin Z, LeJemtel TH, Colombo PC, Feng L. Vascular endothelial sampling and analysis of gene transcripts: a new quantitative approach to monitor vascular inflammation. J. Appl. Physiol. 2008; 103:1873–1878. [PubMed: 17717122]
26. Akiyama SK. Purification of Fibronectin. Curr. Protocols Cell Biol. 1999:10.5.1–10.5.13.
27. Larsen M, Wei C, Yamada KM. Cell and fibronectin dynamics during branching morphogenesis. J. Cell Sci. 2006; 119:3376–3384. [PubMed: 16882689]
28. McKeown-Longo PJ, Mosher DF. Binding of plasma fibronectin to cell layers of human skin fibroblasts. J. Cell Biol. 1983; 97:466–472. [PubMed: 6309861]
29. Daley WP, Gulfo KM, Sequeira SJ, Larsen M. Identification of a mechanochemical checkpoint and negative feedback loop regulating branching morphogenesis. Dev. Biol. 2009; 336:169–182. [PubMed: 19804774]
30. Dubash AD, Menold MM, Samson T, Boulter E, García-Mata R, Doughman R, Burridge K. Chapter 1. Focal adhesions: new angles on an old structure. Int. Rev. Cell Mol. Biol. 2009; 277:1–65. [PubMed: 19766966]
31. Gailit J, Ruoslahti E. Regulation of the fibronectin receptor affinity by divalent cations. J. Biol. Chem. 1988; 263:12927–12932. [PubMed: 2458338]
32. Haas TA, Plow EF. Integrin-ligand interactions: a year in review. Curr. Opin, Cell Biol. 1994; 6:656–662. [PubMed: 7833046]
33. Bazzoni G, Shih DT, Buck CA, Hemler ME. Monoclonal antibody 9EG7 defines a novel β1 integrin epitope induced by soluble ligand and manganese, but inhibited by calcium. J. Biol. Chem. 1995; 270:25570–25577. [PubMed: 7592728]

34. Mendrick DL, Kelly DM. Temporal expression of VLA-2 and modulation of its ligand specificity by rat glomerular epithelial cells in vitro. Lab. Invest. 1993; 69:690–702. [PubMed: 8264232]
35. Pankov R, Cukierman E, Katz BZ, Matsumoto K, Lin DC, Lin S, Hahn C, Yamada KM. Integrin dynamics and matrix assembly: tensin-dependent translocation of α5β1 integrins promotes early fibronectin fibrillogenesis. J. Cell Biol. 2000; 148:1075–1090. [PubMed: 10704455]
36. Mao Y, Schwarzbauer JE. Fibronectin fibrillogenesis, a cell-mediated matrix assembly process. Matrix Biol. 2005; 24:389–399. [PubMed: 16061370]
37. Woods A, Couchman JR. Syndecan-4 and focal adhesion function. Curr. Opin. Cell Biol. 2001; 13:578–583. [PubMed: 11544026]
38. Morgan MR, Humphries MJ, Bass MD. Synergistic control of cell adhesion by integrins and syndecans. Nat. Rev. Mol. Cell Biol. 2007; 8:957–969. [PubMed: 17971838]
39. Beauvais DM, Rapraeger AC. Syndecans in tumor cell adhesion and signaling. Reprod. Biol. Endocrinol. 2004; 2:3–15. [PubMed: 14711376]
40. Beauvais DM, Ell BJ, McWhorter AR, Rapraeger AC. Syndecan-1 regulates αvβ3- and αvβ5-integrin activation during angiogenesis and is blocked by synstatin, a novel peptide inhibitor. J. Exp. Med. 2009; 206:691–705. [PubMed: 19255147]
41. Askari JA, Buckley PA, Mould AP, Humphries MJ. Linking integrin conformation to function. J. Cell. Sci. 2009; 122:165–170. [PubMed: 19118208]
42. Clark K, Pankov R, Travis MA, Askari JA, Mould AP, Craig SE, Newham P, Yamada KM, Humphries MJ. A specific a α5β1-integrin conformation promotes directional integrin translocation and fibronectin matrix formation. J. Cell Sci. 2005; 118:291–300. [PubMed: 15615773]
43. Quantock AJ, Young RD. Development of the corneal stroma, and the collagen-proteoglycan associations that help define its structure and function. Dev Dyn. 2008; 237:2607–2621. [PubMed: 18521942]
44. Ruberti JW, Zieske JD. Prelude to corneal tissue engineering - gaining control of collagen organization. Prog. Retin. Eye Res. 2008; 27:549–577. [PubMed: 18775789]
45. Klotz SA, Penn CC, Negvesky GJ, Butrus SI. Fungal and parasitic infections of the eye. Clin. Microbiol. Rev. 2000; 13:662–685. [PubMed: 11023963]

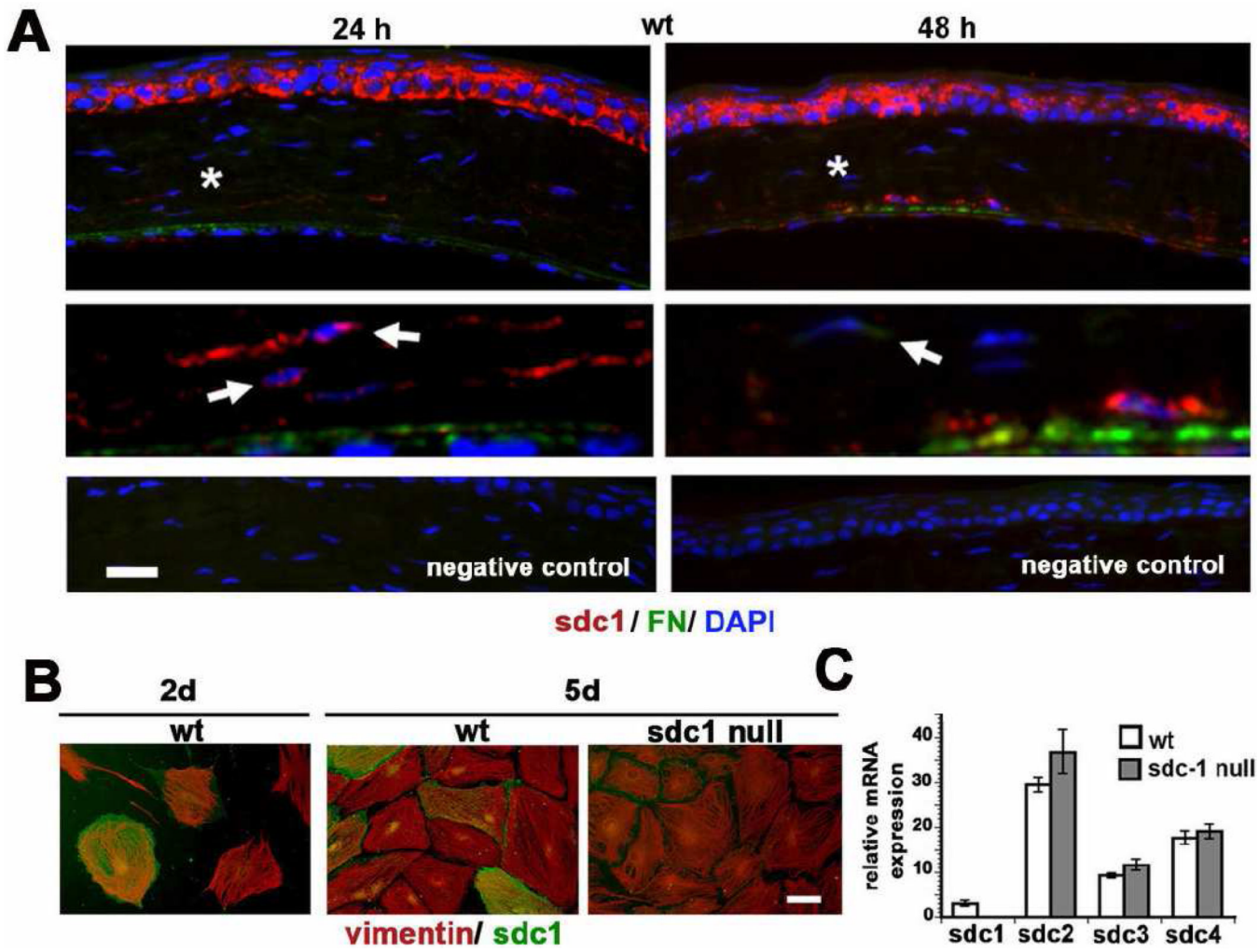

Figure 1. sdc1 on is expressed on corneal stromal fibroblasts in vivo and in vitro

A. Expression of sdc1 and FN can be detected in the CSCs in the posterior cornea 24 and 48 hours after debridement wounds in the wt mouse cornea. Asterisks indicate regions shown magnified three-fold in the panels below with no primary antibody negative control shown in the last row of panels. Note that while sdc1 is present within some cells as indicated by the arrows, it is also observed within the stroma between the collagen lamellae. Extracellular sdc1 is due to shedding of the sdc1 ectodomain and may be derived from either epithelial or stromal cells. **B.** Sdc1 is expressed in a sub-population of wt CSCs at days two and five after being placed in culture. All cells isolated from wt and sdc1 null mice are vimentin positive and assemble vimentin-containing intermediate filament networks that are indistinguishable. **C.** Quantitative RT-PCR was performed on mRNA isolated from wt and sdc1 null CSCs to confirm that sdc1 was absent on the null cells and to look for evidence for compensation for the loss of sdc1 by the up regulation of sdc2, sdc3, and sdc4. Data show that sdc1 is expressed by wt but not sdc1 null CSCs; sdc2, sdc3, and sdc4 are expressed by both genotypes of cells at similar levels. Bars in **A** and **B** equal 20 μm.

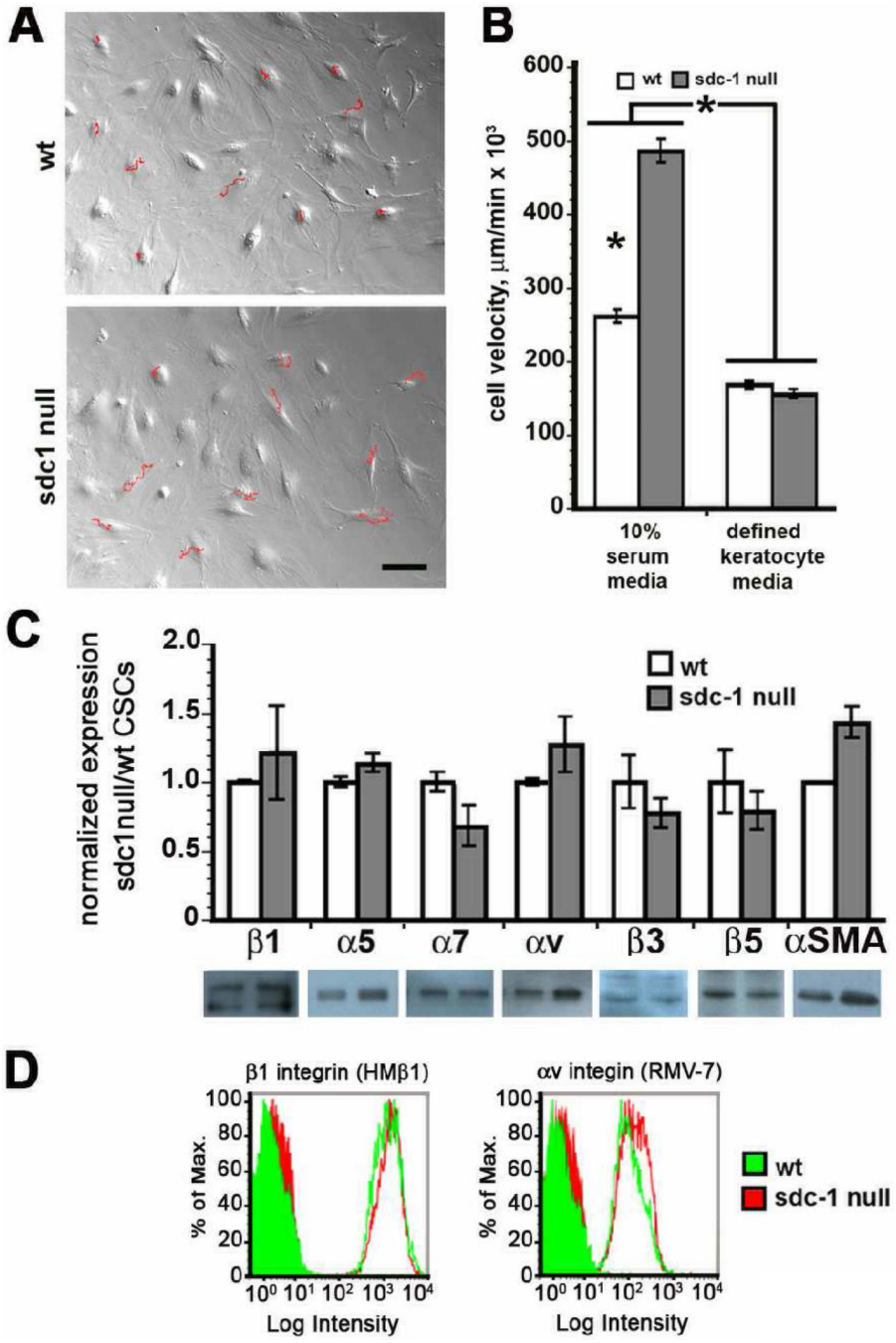

Figure 2. Sdc1 null CSCs migrate faster than wt cells but express similar levels integrins

A. Time-lapse microscopy studies were performed and the tracks of 10 representative cells studied over the 16 hour 40 minute time period are indicated in red. The tracks traveled by sdc1 null cells are longer than those for wt cells. B. The cell velocities were calculated for cells incubated in 10% serum and in defined keratocyte media, which keeps cells in a quiescent state. C. Immunoblots were used for quantification of integrins and αSMA in wt and sdc1 null CSCs. Actin was used as a loading control to calculate the relative expression of each of the proteins shown. Despite a trend for increased expression of αv, α5, and β1 integrins as well as αSMA, data are not significantly different. D. Flow cytometry was performed to evaluate surface integrin expression. There was no difference in the expression

of β1 or αv integrin on wt or sdc1 null CSCs. Filled curves indicate fluorescence intensity as determined using control IgGs and open curves indicate data for the integrin indicated.

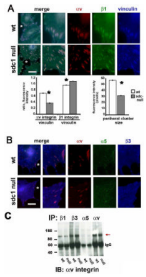

Figure 3. Sdc1 null CSCs assemble focal adhesions containing β1 and αv integrins with less β3 and α5 compared to wt cells

A and **B** show wt and sdc1 null cells grown for two days in culture, fixed, permeabilized, and immunostained for vinculin, αv, and β1 integrin, or for vinculin, α5, and β3 integrin respectively. A region of interest identified with an asterisk in each image was digitally enlarged three-fold and presented with the three molecules stained shown individually and merged. Note that β1 and αv integrins co-localize within focal adhesions in both wt and sdc1 null cells and that these same vinculin-containing focal adhesions show little evidence of β3 and α5 integrin. The line tool was used in Image Pro Plus and the ratios of αv and β1 integrins to vinculin determined; also, the mean intensity of the vinculin-containing clusters in pixels in wt and sdc1 null cells. A minimum of ten cells per variable was assessed and no fewer than 100 ratios calculated per cell. Data are shown for the peripheral adhesions in wt and sdc1 null cells. **C**. Immunoprecipitation of wt and CSC extracts was performed using antibodies against β1, β3, α5 or αv integrins followed by immunoblotting with αv integrin to reveal the presence of αvβ1 integrin heterodimers within CSC extracts. αv is immunoprecipitated using antibodies against β1, β3, and αv integrins but not α5 (red arrow). The asterisks in the bar graphs in A indicate data that are significant by ANOVA with p values < 0.05 and the bar in A and B = 10 μm.

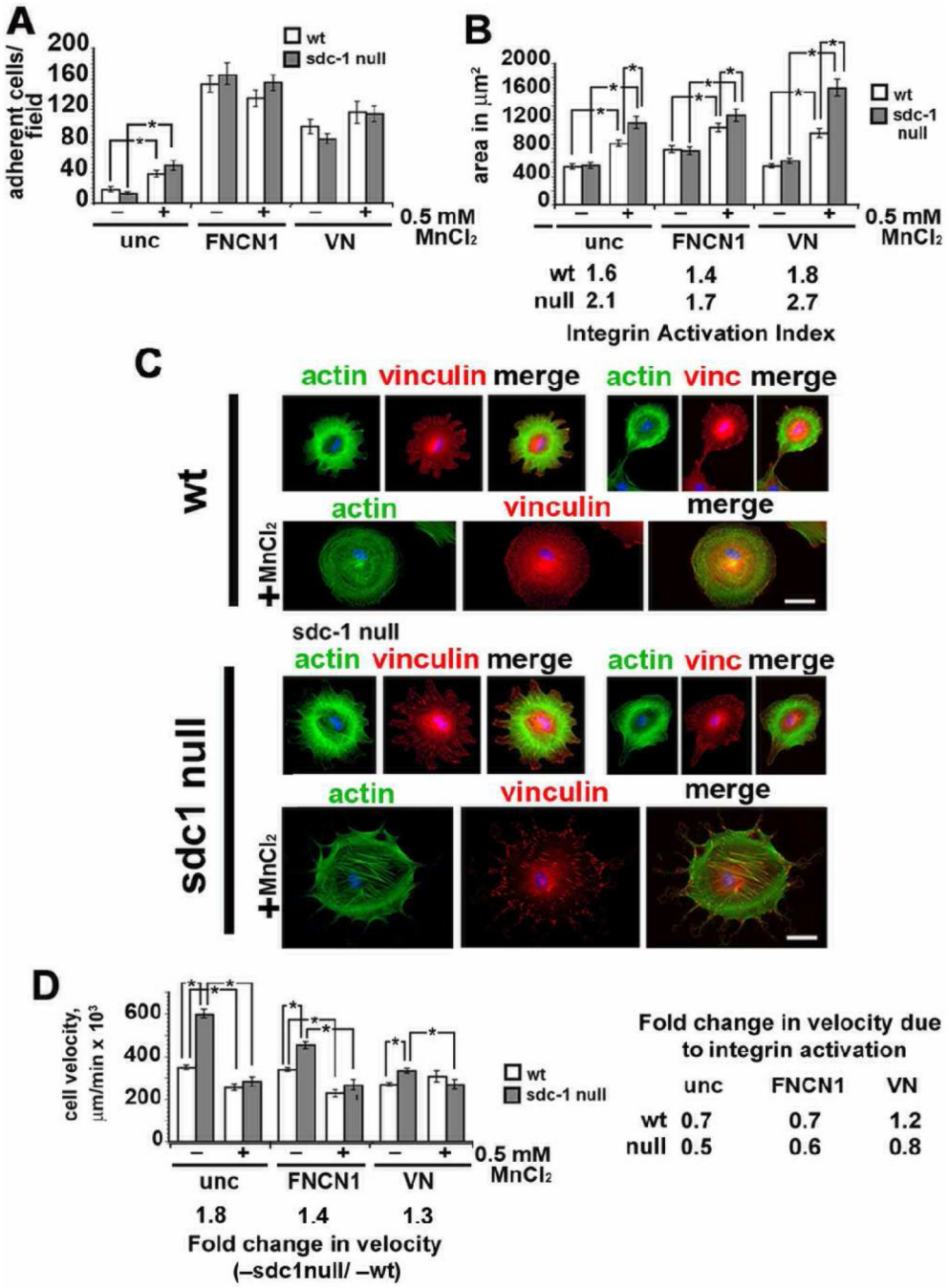

Figure 4. Integrin activation of CSCs with divalent cations induced extracellular matrix-dependent differences in sdc1 null cell adhesion and spreading but reduced cell migration differences between wt and sdc1 null cells

A. CSCs were adhered for 1 hour to uncoated, FNCN1-, or VN-coated with and without $MnCl_2$ treatment and the numbers of cells that attached were determined. **B. and C.** CSCs were adhered to uncoated, FNCN1-or VN-coated surfaces for 20 min and media replenished with or without $MnCl_2$ and cells were allowed to spread for four hours. The $MnCl_2$-induced integrin activation index (spread area of $MnCl_2$ treated/spread area for untreated cells) was calculated for a minimum of 80 cells per variable and is indicated above the bars for the $MnCl_2$-treated cells in panel **B**; in panel **C**, immunostaining is shown for actin filaments

(green) and vinculin (red) to identify focal adhesions for cells spreading on uncoated surfaces. Note the larger size of the $MnCl_2$-treated sdc1 null cells and their larger focal adhesions in comparison with wt cells. **D.** Time-lapse microscopy studies indicate that sdc1 null cells migrate faster than wt cells when replated onto uncoated tissue culture plastic, FNCN1, or VN respectively; fold differences in the migration rates of untreated sdc1 null compared to wt cells are shown below the graph. When $MnCl_2$ was added to cultures, sdc1 null CSC migration rates were reduced such that both genotypes migrated at the same rate. The data to the right of the graph show the fold-change in velocity induced by $MnCl_2$ treatment on each of the substrates tested. Asterisks indicate data that are statistically significant by AVOVA. Scale bar shown in **C** = 20 μm.

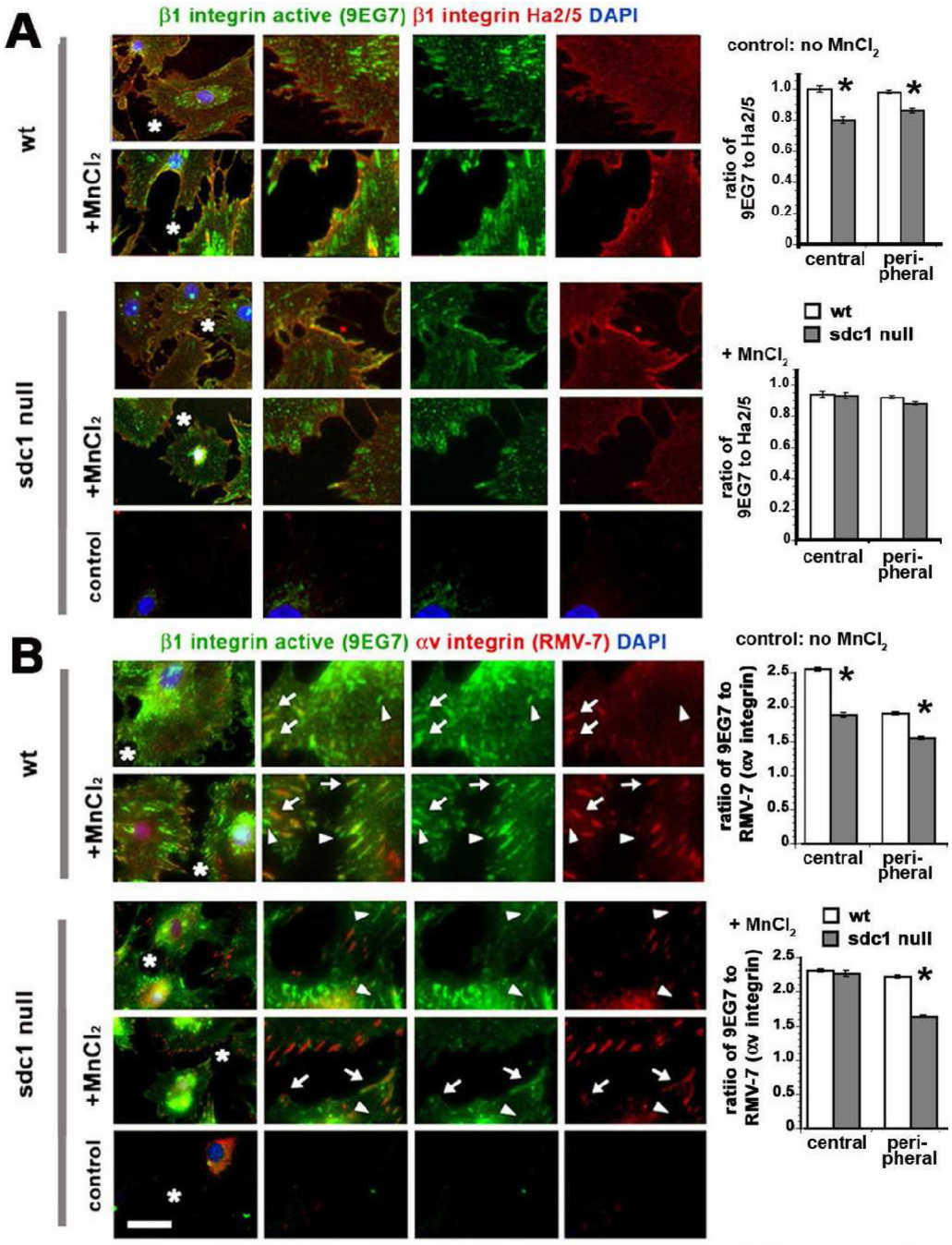

Figure 5. CSCs lacking sdc1 express less activated β1 integrin-positive fibrillar and focal adhesions

CSCs were grown overnight and then treated with $MnCl_2$ for 24 hours. Cells were fixed and immunostained without permeabilization using either **(A)** the activation dependent β1 integrin antibody 9EG7 and the function blocking β1 integrin antibody Ha2/5 or (**B**) the FITC-conjugated 9EG7 activation dependent β1 integrin antibody and the biotinylated function blocking αv antibody RMV-7. DAPI was used to reveal nuclei. A region of interest indicated by a white asterisk in each image on the left was digitally enlarged to three times its original size. Integrins are shown individually on the right and merged. The arrows in B highlight clusters positive for both activated β1 integrin and αv integrin; the arrow heads

indicate clusters positive for activated β1 integrin but not αv integrin. The controls shown are secondary antibody controls for **A** and irrelevant FITC-conjugated IgG and Alexa 594-conjugated streptavidin for **B**. The graphs indicate in **A**, the ratios of activated β1 integrin obtained using 9EG7 to β1 integrin obtained using Ha2/5 and, in **B**, the ratios of activated β1 integrin obtained using 9EG7 to αv integrin obtained using RMV-7. A minimum of ten cells per variable was assessed and no fewer than 100 ratios calculated per cell. The black asterisks on the graphs indicate data that are significant by ANOVA with $p < 0.05$. Scale bar in A and B equals 10 μm.

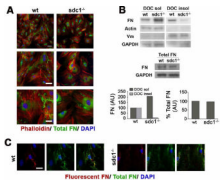

Figure 6. CSCs lacking sdc1 synthesize the same amount of FN but assemble fewer DOC-insoluble FN fibrils

A. Wild type and sdc1-null CSC were cultured for five days and immunostained with an antibody specific for endogenous FN. Sdc1-null CSCs exhibit fewer endogenous FN fibrils (green) than their wild type counterparts. Staining for F-actin (phalloidin, red) and nuclei (DAPI) are also shown. **B.** Sdc1 null CSCs exhibit increased DOC soluble and decreased DOC insoluble FN relative to wild type CSCs. Quantification of CSC DOC soluble and insoluble extracts was normalized to levels of β-actin and vimentin, respectively, and expressed relative to wild type CSCs. Vimentin (DOC insoluble) and β-actin (DOC soluble) confirmed separation of the two fractions. In contrast, wild type and sdc1-null CSCs exhibit no difference in the amount of total endogenous FN, with quantification normalized to GAPDH. Shown is one representative experiment of three. **C.** Sdc1 null CSCs also incorporate less exogenous FN into a fibrillar matrix (red), shown relative to the endogenous matrix (green). The scale bar in A for the top images is 100 μm and is 40 μm for the lower images; in C, the bar is 20 μm. Wt and sdc1 null cells are shown at the same magnification.

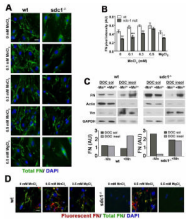

Figure 7. $MnCl_2$ treatment of sdc1 null cells reverts the FN fibrillogenesis phenotype to that of wt cells

A. Wild type and sdc1 null CSCs were treated with either increasing concentrations of $MnCl_2$ followed by immunostaining for endogenous FN. $MgCl_2$ was used as a negative control. Both genotypes assemble an increased number of endogenous FN fibrils (green) in the presence of $MnCl_2$, but not $MgCl_2$. Nuclei, detected with DAPI, are shown in blue. **B.** Quantification of total FN pixel intensity, normalized to nuclear staining, from at least five representative images from the experiment shown in (A) reveal that increasing concentrations of $MnCl_2$, but not $MgCl_2$, revert the FN fibrillogenesis phenotype of sdc1 null CSCs to that of the wild type cells. **C.** DOC extractions of wild type and sdc1-null CSCs cultured in the presence and absence of $MnCl_2$ reveal that both wild type and sdc1 null cells exhibit decreased amounts of DOC-soluble FN and increased amounts of DOC-insoluble FN when cultured with $MnCl_2$ but that this effect is more pronounced for sdc1 null cells. Quantification was performed as in Fig 5B, and β-actin (DOC soluble) and vimentin (DOC insoluble) were used to assess separation quality. **D.** Sdc1 null CSCs cultured with increasing concentrations of $MnCl_2$ incorporate similar amounts of fluorescent FN added exogenously to cells during culture into fibrillar matrices as their wild type counterparts. Fluorescent FN (red) is shown relative to the total FN (green). ANOVA, *p<0.05, **p<0.01, ***p<0.001, N=5. Scale bars, 20 μm (A, D, and E).

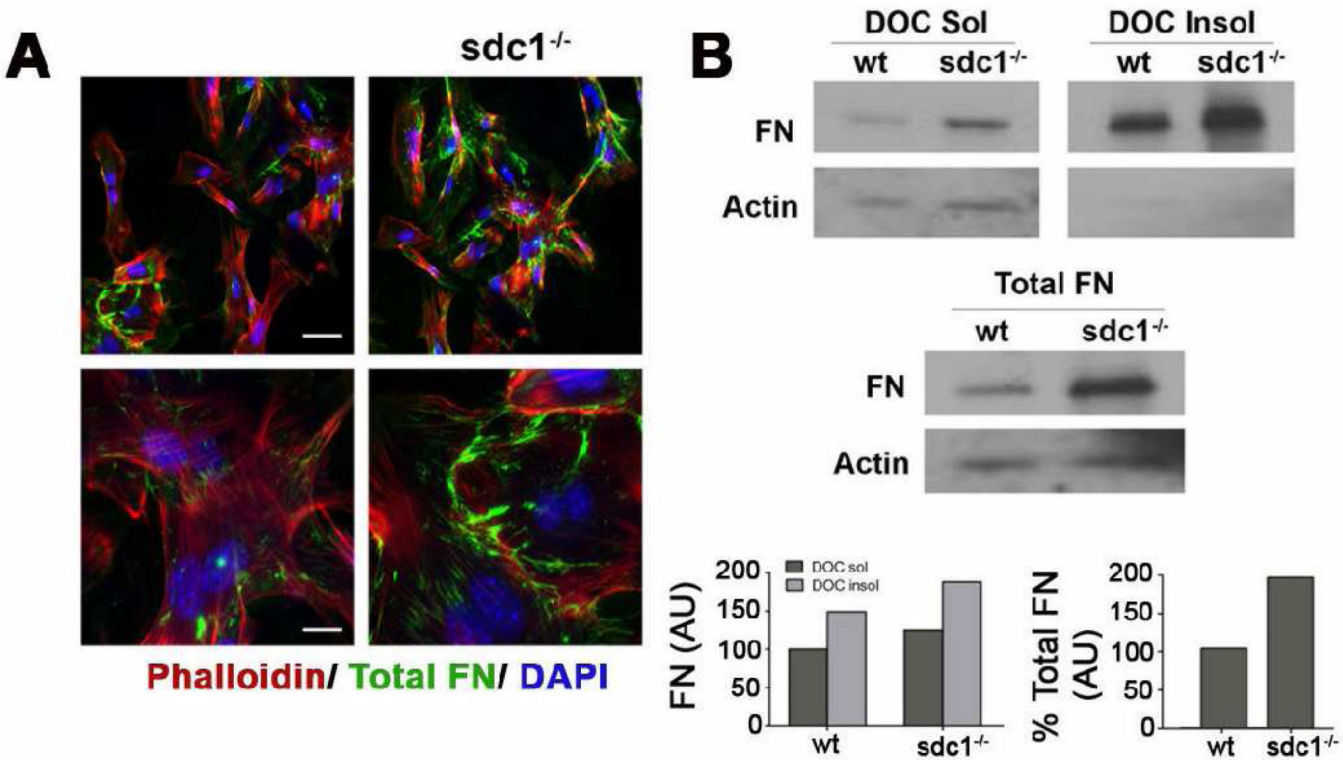

Figure 8. Dermal fibroblasts lacking sdc1 synthesize increased levels of FN and assemble DOC-insoluble FN fibrils

A. Wild type and sdc null dermal fibroblasts were immunostained for total FN (green); actin (red) and nuclei (blue) were visualized with rhodamine phalloidin and DAPI, respectively. Both wild type and sdc1 null dermal cells assemble FN fibrils at the cell surface. **B.** Sdc1 null dermal fibroblasts exhibit both increased DOC-soluble and insoluble FN relative to wild type dermal fibroblasts. Sdc1 null dermal fibroblasts also expressed more total FN than their wild type counterparts. Quantification is expressed relative to actin and to wild type dermal fibroblasts. Shown is a representative blot and quantification of that blot for each experiment. Scale bars, 40 μm and 20 μm (A).

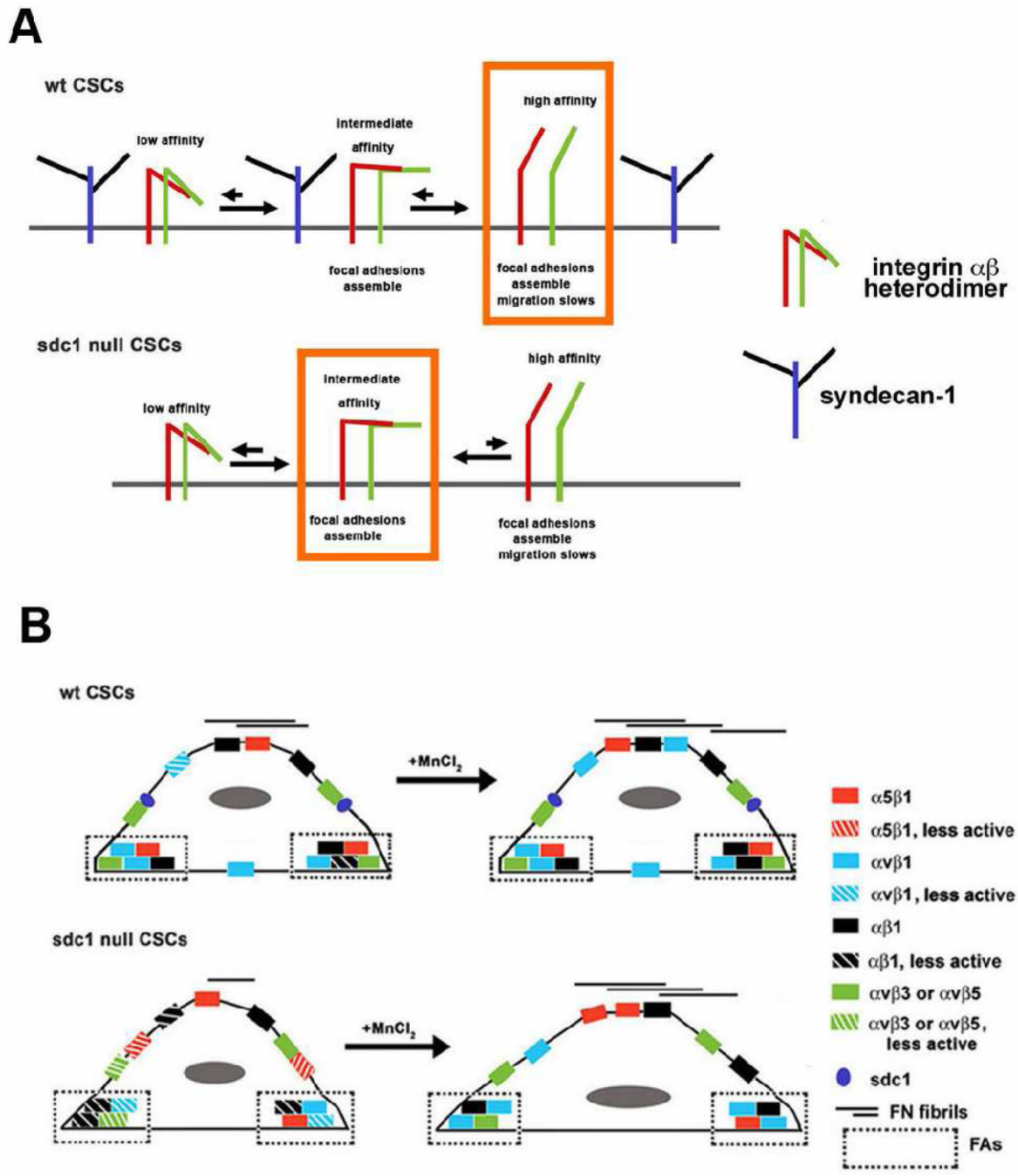

Figure 9. Proposed model for how integrin activation and FN fibillogenesis are regulated by sdc1 in CSCs

A shows schematically the roles we hypothesize that that sdc1 plays in regulating integrin activation. We propose that sdc1 directly or indirectly promotes activation of integrins which leads to moderate rates of cell migration and optimal FN fibrillogenesis. The orange boxes show the primary integrin activation state observed in wt and sdc1 null cells. $MnCl_2$ further activates integrins and enhances FN fibril formation. Since integrins do cluster within FAs in sdc1 null cells, the α and β integrin cytoplasmic domains must separate in sdc1 null cells to allow talin, vinculin and other focal adhesion scaffold proteins to bind and cluster. Inside-out integrin signaling also involves movement of the two integrin

cytoplasmic tails away from one another; it is accompanied by the pivoting of the head domains and ligand binding. In sdc1 null cells, despite the clustering, the integrins within their focal and fibrillar adhesions remain inactive unless the cells are treated with $MnCl_2$. **B** shows that upon $MnCl_2$ activation, the sdc1 null cells spread more, they migrate slower, and they accumulate more FN fibrils on their surface. Integrins with intermediate activity support more rapid migration and reduced FN-fibrillogenesis.

Table 1

Antibodies used for these studies

Antigen	Source	Catalog # / Name	Application*
Integrin			
α5 integrin	Millipore, Temecula, CA	AB1928	IB, IP
α7 integrin	Santa Cruz Biotech, Santa Cruz, CA	sc-27710	IB
αv integrin	Millipore	AB1930	IB, IP
αv integrin	BioLegend	104105	FC
αv integrin (RMV-7)	BioLegend	104103	IFs
αv integrin (RMV-7)	BD Biosciences, San Jose, CA	552299	IFs, IFp
β1 integrin	Marcantonio and Hynes [22]	363K	IBAIP
β1 integrin	Sta.Iglesia et al. [23]	Rab27	IB, IP, IFp
β1 integrin (HMβ1)	BioLegend	102205	FC
β1 integrin (9EG7)	BD Biosciences	553715	IFs
β1 integrin (Ha2/5)	BD Biosciences	555003	IFs
β3 integrin	Millipore	AB1932	IB, IP
β5 integrin	Millipore	AB1926	IB
Other			
αSMA	Sigma-Aldrich, St.Louis, MO	63103	IB
β-actin	Millipore	MAB1501R	IB
FN antibody	Dr. K.M. Yamada, NIH	R5836	IFp
phalloidin	Molecular Probes, Eugene, OR	41A1-4	IFp
sdc1	BD Pharmingen	281-2	IB
vimentin	Millipore	AB5733	IFp
vinculin	Millipore	MAB3574	IFp

*IB–Immunoblot; IP–Immunoprecipitation; IBAIP –Immunoblot after immunoprecipitation; IFs–Immunofluorescence-surface, non-permeabilized; IFp–Immunofluorescence-permeabilized; FC–flow cytometry